Demixing and crystallization of DODAB in DPPC–DODAB binary mixtures

ARTICLE *in* PHYSICAL CHEMISTRY CHEMICAL PHYSICS · JUNE 2014

Impact Factor: 4.49 · DOI: 10.1039/c4cp01707b · Source: PubMed

5 AUTHORS, INCLUDING:

Fu-Gen Wu
Southeast University (China)
41 PUBLICATIONS **359** CITATIONS
SEE PROFILE

Zhi-Wu Yu
Tsinghua University
103 PUBLICATIONS **1,674** CITATIONS
SEE PROFILE

PCCP

PAPER

Demixing and crystallization of DODAB in DPPC–DODAB binary mixtures

Cite this: *Phys. Chem. Chem. Phys.*, 2014, **16**, 15307

Fu-Gen Wu,[ab] Rui-Guang Wu,[c] Hai-Yuan Sun,[a] Yan-Zhen Zheng[a] and Zhi-Wu Yu*[a]

Received 19th April 2014,
Accepted 7th June 2014

DOI: 10.1039/c4cp01707b

www.rsc.org/pccp

The crystallization mechanism of one lipid component within multicomponent lipid mixtures remains unclear. To shed light on this issue, we studied the demixing and crystallization behaviors of a binary lipid system using neutral dipalmitoylphosphatidylcholine (DPPC) and cationic dioctadecyldimethylammonium bromide (DODAB) as model molecules. The results indicate that when DODAB is no more than equimolar (*e.g.*, DPPC/DODAB = 2/1 and 1/1), DPPC is miscible with DODAB and hinders the crystallization of DODAB, and the samples undergo reversible gel–fluid phase transitions upon heating and cooling. However, when DODAB is dominant in the mixture (DPPC/DODAB = 1/2), cooling of the mixed fluid phase results in the formation of a DODAB-rich gel domain and a DPPC–DODAB mixed gel domain. Such phase-separated mixed gels can undergo further demixing and crystallization, producing a DODAB-rich crystalline domain and a DPPC-rich tilted gel domain upon prolonged (or plus low-temperature) incubation. Besides, evidence has been given that the crystallized DODAB-rich domain remains in the same lipid bilayer as the DPPC-rich domain. All the three binary lipid mixtures can hold large amounts of water in the lipid interlamellar regions, allowing the incorporation of a large number of water-soluble substances such as DNA or proteins, which can be used for the fabrication of functional biofilms and biomaterials. Influences of water content and salt concentration on the phase structures (*e.g.*, repeat distances) of the binary mixtures have also been studied.

1. Introduction

Lipoplexes, the complexes of DNA and cationic lipids, have been widely studied because of their potential use as nonviral gene delivery systems.[1–10] Here, DNA is packed in various organized lipid structures such as lamellar and hexagonal phases.[11–14] The lamellar phase consists of smectic-like arrays of stacked lipid bilayers with DNA monolayers intercalated within the water gaps.[3,15] For the lipid matrix, the cationic lipid is usually mixed with a helper lipid (often a zwitterionic lipid) to enhance transfection potency and to reduce toxicity.[16–23] Although there have been many investigations on the lipoplexes, a detailed molecular picture on the organization of the lipid matrix is still not available. A deeper understanding of the properties of the lipid matrix, therefore, is in urgent need. Generally speaking, the shape and stability of lipoplexes depend largely on the chemical composition and physical properties of the lipids constituting the complex.[24] And the DNA delivery efficiency of lipoplexes is found to be mainly influenced by the features of the involved lipids.[25,26] Thus, studies regarding the lipid matrix could be crucial to find optimal lipid phases for transfection[27] and may even lead to overcome the efficiency limit of nonviral DNA delivery pathways.[24]

For the lipid matrix, some important questions such as the structure, phase stability, phase separation, and domain or defect formation may arise. There have been several recent attempts aiming at elucidating the structure and phase state of the binary lipid mixtures. A recent work[28] found that the zwitterionic distearoylphosphatidylcholine (DSPC) and cationic dihexadecyldimethylammonium bromide (DHDAB) mixed monolayer at $x_{DHDAB} = 0.3$ exhibits the tightest intermolecular packing. The most stable composition against aggregation for the DSPC–DHDAB mixed vesicles, however, was found at $x_{DHDAB} = 0.5$. For the lipid mixture consisting of cationic dimyristoyltrimethylammonium propane (DMTAP) and zwitterionic dimyristoylphosphatidylcholine (DMPC), both experimental[29] and simulational[30] results revealed that the average area per lipid of the monolayer or bilayer reaches minimum at a mole fraction of about 50% cationic lipid. For a similar system composed of DMPC and dioleoyloxytrimethylammonium propane (DOTAP),[31] the minimal molecular area of the mixed bilayer was observed at a lower TAP fraction of 0.4. Adding unsaturated DOTAP lipids into DMPC bilayers was found to promote lipid chain interdigitation

[a] *Key Laboratory of Bioorganic Phosphorous Chemistry and Chemical Biology (Ministry of Education), Department of Chemistry, Tsinghua University, Beijing 100084, P. R. China. E-mail: yuzhw@tsinghua.edu.cn*
[b] *State Key Laboratory of Bioelectronics, School of Biological Science and Medical Engineering, Southeast University, Nanjing 210096, P. R. China*
[c] *School of Chinese Materia Medica, Beijing University of Chinese Medicine, Beijing 100102, P. R. China*

and to fluidize lipid bilayers, as seen through enhanced lateral lipid diffusion. Moreover, the thermotropic phase behavior of DPPC and dipalmitoyltrimethylammonium propane (DPTAP) mixtures has also been studied and the results revealed that the equimolarly mixed sample shows the highest transition temperature upon heating.[32] Besides, TAP was found to cause significant reorientation (from more parallel to the membrane plane to more perpendicular) of the P–N dipole vector of the PC headgroup[22,30,32] and lateral polarization of neighboring PC molecules.[33] There have also been studies on solid supported lipid bilayers consisting of zwitterionic and cationic lipid mixtures. One example is the observation of a hexagonal supercrystal phase consisting of DSPC and DOTAP.[34] Besides, it was found that mixing DMPC with up to 20 mol% DMTAP produces a defect-free gel-phase in supported lipid bilayers.[35]

We are interested in studying the phase stability and phase separation/domain formation in the mixed cationic–zwitterionic lipid bilayers, especially the crystallization process of one lipid component within the binary lipid mixtures. To address these issues, we selected the cationic lipid dioctadecyldimethylammonium bromide (DODAB) to mix with the zwitterionic DPPC to form a lipid binary system. The simple, inexpensive and synthetic cationic lipid DODAB (and its analogue, dioctadecyldimethylammonium chloride, DODAC) has many applications in drug and vaccine delivery.[36–39] Several previous studies have revealed that the neat DODAB molecules can undergo crystallization under certain conditions.[40–42] For DPPC–DODAB binary mixtures, the phase behavior of DPPC–DODAB monolayers[43] and vesicles[44,45] have been characterized. Besides, the adsorption behaviors of DPPC–DODAB mixtures onto surfaces of solid particles have also been investigated.[46,47] Regarding the stability of DPPC–DODAB mixtures, it was reported that an equimolar mixture of DPPC and DODAB shows a higher melting temperature than each of the pure components.[44] This result was further studied and confirmed by molecular dynamics simulation[30] and by mean-field calculations.[22] The work by Carmona-Ribeiro *et al.* also reported that at 50% DODAB, the colloidal stability of DPPC–DODAB vesicles is the highest: a maximum phase transition temperature was observed and the vesicles can be stable at NaCl concentrations of 150 mM.[45] Although the above investigations have addressed some issues of the DPPC–DODAB system, a detailed and multi-angle understanding of the structure and phase transition mechanisms, especially the phase stability and phase separation/domain formation issues of this system, still remains elusive and needs to be characterized. We will use this system as a model to study how one component demixes and crystallizes within multicomponent mixtures.

The present study is a continuation of our efforts in understanding the formation mechanisms of crystal phases in lipid systems. Except DODAB, we have also investigated the crystallization of other lipids. For example, the critical role the water molecules played in the transition of a metastable crystalline phase to a stable crystallization phase has been demonstrated for dilauroylphosphoethanolamine (DLPE) bilayers.[48] The critical role of the hydrocarbon tails in triggering the phase transition from the gel phase to the crystallization phase of DPPC bilayers has also recently been proven experimentally.[49] Besides, some other groups have also studied the crystallization behavior of negatively charged phosphatidylserine (PS) membranes by X-ray scattering[50] and molecular dynamics (MD) simulation.[51] These above mentioned studies all focused on the investigation of a single lipid component system. Herein, we intended to uncover the crystallization details of one lipid component within a binary lipid mixture using the DPPC–DODAB mixtures as a binary lipid model.

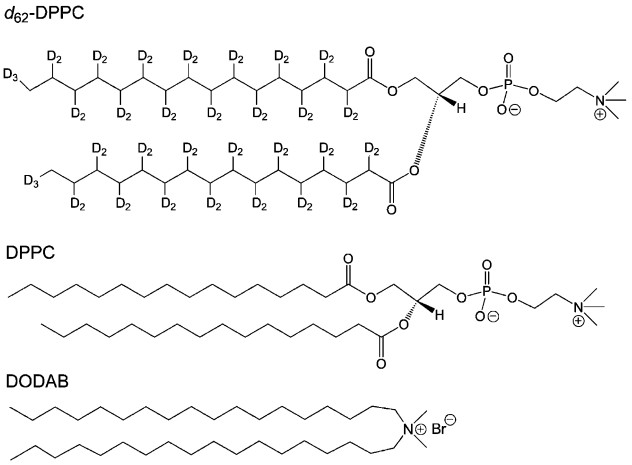

Fig. 1 The molecular structures of d_{62}-DPPC, DPPC and DODAB.

In this work, we have studied the structure and phase transition mechanisms of the DPPC–DODAB binary mixtures by using conventional and high-sensitivity differential scanning calorimetry (DSC and microDSC), synchrotron small- and wide-angle X-ray scattering (SAXS and WAXS) and Fourier transform infrared (FTIR) spectroscopy. In the temperature-scanning FTIR experiments, to study the rearrangements of the lipid hydrocarbon chains of the DPPC and DODAB molecules independently, a deuterated lipid, 1,2-dipalmitoyl-d_{62}-*sn-glycero*-3-phosphocholine (d_{62}-DPPC), was used instead of the hydrogenated DPPC. Fig. 1 illustrates the molecular structures of the three lipid molecules (d_{62}-DPPC, DPPC and DODAB) used in this work.

2. Experimental section

2.1. Sample preparation

DPPC and d_{62}-DPPC was purchased from Avanti Polar Lipids Inc. (Birmingham, AL). DODAB with purity better than 99% was purchased from Acros Organics (Belgium). The weighed amounts of DPPC (or d_{62}-DPPC) and DODAB were solubilized in chloroform. The solvent was evaporated under a stream of nitrogen and was then placed in a vacuum for more than 12 h to remove the residual solvent. Double deionized H_2O with a resistivity of 18.2 MΩ cm was then added to the obtained DPPC–DODAB or d_{62}-DPPC–DODAB mixture. The concentrations of the total lipid mixture are 25 wt% and 1 mg mL^{-1} (0.1 wt%) in the conventional DSC and microDSC measurements, respectively. For the concentrated sample (25 wt%), homogeneous lipid dispersions were prepared by cycling the

samples at least four times between 20 and 80 °C. For the dilute lipid sample (1 mg mL^{-1}), homogeneous lipid dispersions were prepared by stirring the mixture at 70 °C for 1 h. After that, different sample storage methods were used to modulate the phase behavior of the binary lipid mixtures.

2.2. DSC

For the microDSC experiment, the calorimetric measurements were performed on a CSC Model 6300 Nano III differential scanning calorimeter (Calorimetry Sciences Corp., Lindon, UT) using the DSCRun software. The scan rate was 0.5 °C min^{-1}.

Conventional DSC data of the concentrated lipid samples were obtained using a differential scanning calorimeter DSC821e equipped with a high-sensitivity sensor HSS7 (Mettler-Toledo Co., Switzerland). The scan rate was also 0.5 °C min^{-1}.

2.3. Synchrotron X-ray diffraction

SAXS and WAXS experiments were performed at the beamline BL16B1 of the Shanghai Synchrotron Radiation Facility (SSRF) (λ = 1.24 Å). A Rayonix SX-165 CCD detector was used to collect the X-ray scattering data. X-ray scattering intensity patterns were recorded during 120 s exposure of the samples to the synchrotron beam. To acquire the SAXS data, we adjusted the sample-to-detector distance to 1.8 m, while to obtain the WAXS data, we fixed the sample-to-detector distance at 0.5 m. A standard silver behenate sample was used for the calibration of diffraction spacings. A Linkam thermal stage (Linkam Scientific Instruments, the United Kingdom) was used for temperature control (±0.1 °C). The X-ray powder diffraction intensity data were analyzed using the program Fit2D.

2.4. FTIR spectroscopy

FTIR spectra were recorded using a Nicolet 5700 Fourier transform infrared spectrometer with a DTGS detector in the range of 4000–900 cm^{-1} with a spectral resolution of 2 cm^{-1} and a zero filling factor of 2. Samples were coated onto the inner surfaces of a pair of CaF_2 windows, which were mounted on a Linkam heating–cooling stage for temperature control (±0.1 °C). Spectra were recorded every ~30 s and each spectrum consists of 16 scans.

3. Results and discussion

3.1. DSC and synchrotron X-ray scattering

We will first show the DSC results (Fig. 2–4) since they can give a rough picture of the phase behavior of the DPPC–DODAB binary mixtures. The details regarding the identification of the different phase states will be presented later with the help of the synchrotron X-ray scattering data (Fig. 5–7). Fig. 2 shows the microDSC results of the three binary mixtures with the total lipid concentration of 1 mg mL^{-1}. For DPPC/DODAB = 2/1 (Fig. 2A) and 1/1 (Fig. 2B) samples, their immediate reheating scans both give a single endothermic peak at T_{peak} = 55 °C and 57 °C, respectively, corresponding to a gel to fluid phase transition process. The heating scans of the two samples after incubation at 20 °C for 30 days or after incubation at −20 °C for 2 days and then

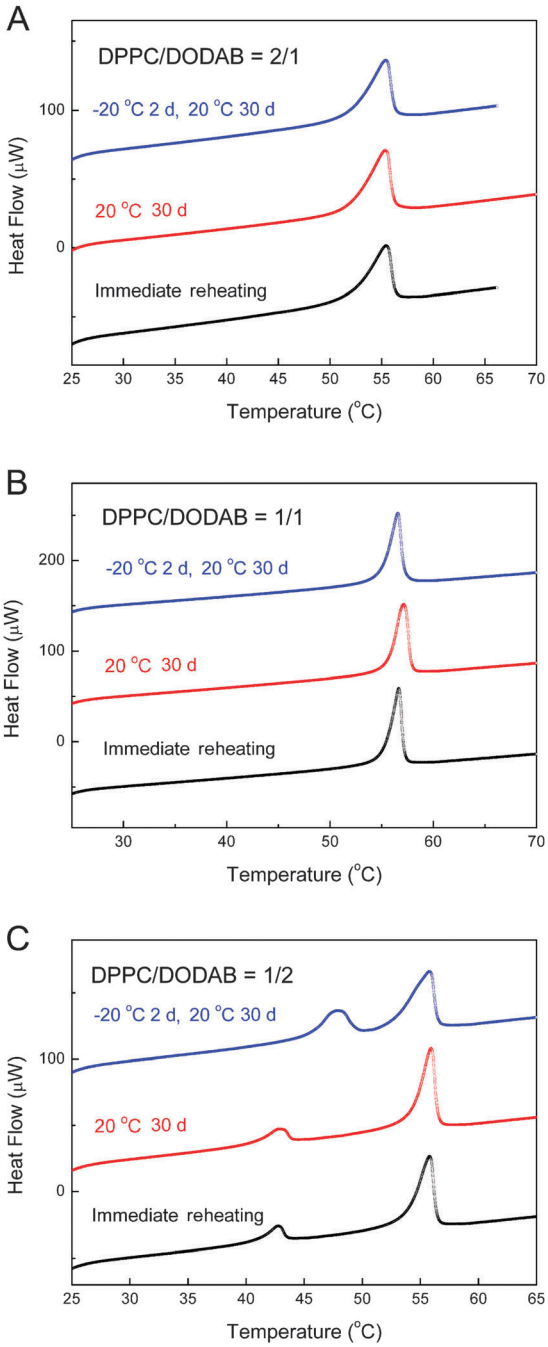

Fig. 2 microDSC results for the dilute (1 mg mL^{-1}) DPPC/DODAB samples with different thermal histories as labeled. (A) DPPC/DODAB = 2/1, (B) DPPC/DODAB = 1/1, (C) DPPC/DODAB = 1/2.

at 20 °C for 30 days show almost identical DSC results as those of their corresponding immediate reheating scans. These results show that the 2/1 and 1/1 samples have very similar phase transition behaviors after various thermal treatments.

For DPPC/DODAB = 1/2 sample, the immediate reheating scan of the sample cooled from 70 °C to 20 °C gives two endothermic peaks at 43 °C and 56 °C (Fig. 2C). This indicates that the sample before heating is in a phase-separated state. If the sample cooled from 70 °C to 20 °C was incubated at 20 °C

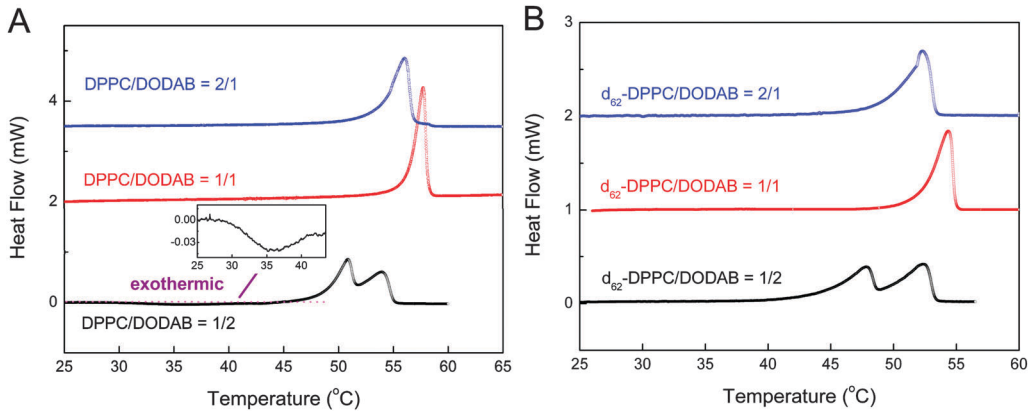

Fig. 3 Conventional DSC results for the concentrated (25 wt%) DPPC–DODAB (A) and d_{62}-DPPC–DODAB (B) binary mixtures. The inset in (A) is the enlarged curve for the exothermic peak. Before measurements, these samples were first incubated at −20 °C for 2 days and then stored at 20 °C for 14 days.

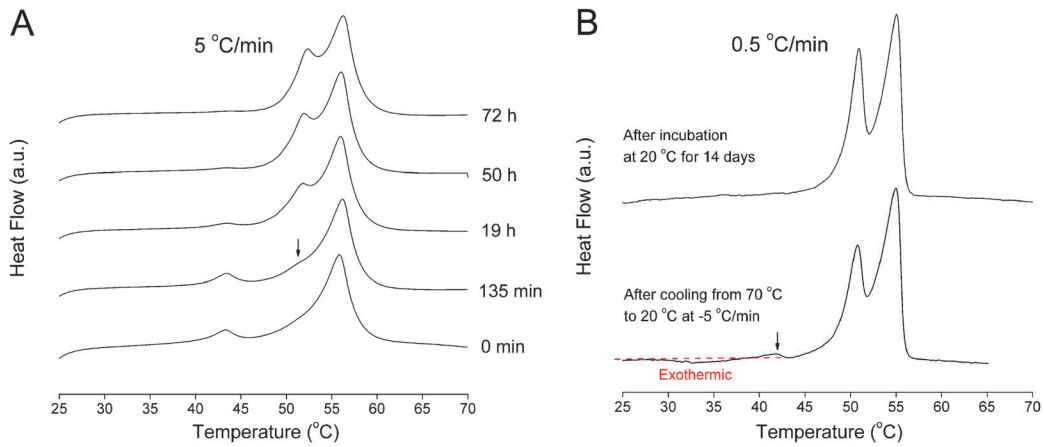

Fig. 4 Conventional DSC results for the DPPC/DODAB = 1/2 aqueous dispersion (total lipid content = 25 wt%). (A) Before measurements, the samples were cooled from 70 °C to 20 °C at −5 °C min^{-1} and incubated at 20 °C for different periods of time as indicated. The heating rate was 5 °C min^{-1}. (B) Before measurements, the samples were cooled from 70 °C to 20 °C at −5 °C min^{-1} followed by no incubation (the lower curve) or incubation for 14 days (the upper curve). The heating rate was 0.5 °C min^{-1}.

for 30 days, the microDSC scan result is almost the same as that of the immediate reheating scan. However, if the sample was cooled from 70 °C to −20 °C, incubated at the same temperature for 2 days and then stored at 20 °C for 30 days, two peaks at 48 °C and 56 °C are seen on the following heating scan curve. This means that the additional low-temperature incubation procedure (−20 °C for 2 days) significantly changed the phase state as compared with that of the sample incubated at 20 °C for 30 days. The reasons why the special crystallization condition of "−20 °C 2 days and 20 °C 30 days" was chosen are as follows: according to the common crystallization theory, the crystal nuclei formation needs a low temperature period, while the crystal growth process needs a relatively high temperature (but below the melting transition temperature) to gain enough energy for adjusting the packing of the molecules.

Fig. 3 shows the conventional DSC results of the three binary lipid mixtures with the total lipid concentration of 25 wt%. These samples were prepared by first incubating at −20 °C for 2 days and then at 20 °C for 14 days. For the DPPC–DODAB binary mixtures (Fig. 3A), the 2/1 and 1/1 samples give only one endothermic peak at 56 and 58 °C, respectively, upon heating. The reheating scans generated almost identical results (data not shown). These results are nearly the same as those of the dilute samples shown in Fig. 2, suggesting that the concentration of the samples do not affect their corresponding phase behaviors. The 1/2 sample, however, gives two endothermic peaks centered at 51 °C and 54 °C, which are very similar to the two-peak pattern observed for the corresponding dilute 1/2 sample treated at low temperature (−20 °C) as shown in Fig. 2C. We should also mention that from the DSC results of both the dilute and concentrated samples, the 1/1 sample shows the highest thermostability in the three investigated molar ratios, which is in good agreement with the previous work.[45]

Since the DSC results for the dilute and concentrated samples are very similar, only the concentrated samples were chosen for further phase state identification by the synchrotron X-ray scattering technique. For the DPPC/DODAB = 2/1 sample (Fig. 5), the single, sharp WAXS peak at 14.6 nm^{-1} at 20 °C

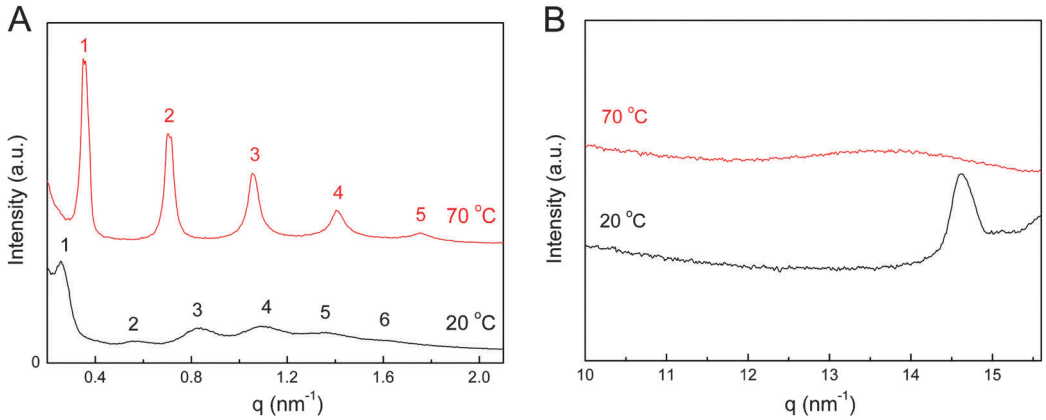

Fig. 5 SAXS (A) and WAXS (B) results of DPPC/DODAB = 2/1 (total lipid content = 25 wt%). Before measurements, these samples were first incubated at −20 °C for 2 days and then stored at 20 °C for 14 days.

shows that the hydrocarbon chains of DPPC and DODAB molecules are in a gel-state packing (Fig. 5B). Upon heating to 70 °C, both DPPC and DODAB molecules are in the fluid phase with a very broad WAXS peak at ~13.7 nm^{-1} (Fig. 5B). For SAXS data (Fig. 5A), the vectors at the scattering maxima (q_m) show a ratio of 1 : 2 : 3 : 4 : 5 : 6 for the samples at 20 and 70 °C, indicating that the sample at the two temperatures are both lamellar-structured. From the q values, we can obtain the repeat distances (the d values) using the equation $d = 2\pi/q$. The thus obtained average d value is 21.9 nm at 20 °C and 16.4 nm at 70 °C. For the DPPC/DODAB = 1/1 sample (Fig. 6), the results are similar to those of the 2/1 sample. The only difference is that the lamellar repeat distance is 20.5 nm and 15.8 nm for the samples at the gel phase (20 °C) and the fluid phase (70 °C), respectively. For both 2/1 and 1/1 samples, we can see that the SAXS peaks in the gel phase are much broader than those in the fluid phase. The sharpness or width of a SAXS peak collected for a multilamellar vesicular dispersion can reflect the regularity of the bilayer stacking. A sharp peak corresponds to the regular stacking of lipid bilayers, while a broad peak relates to an irregular stacking of the lipid bilayers. The SAXS peaks at 20 °C is much broader than that at 70 °C, indicating that the bilayer stacking in the fluid phase is more regular than that in the gel phase. This may be due to the rigidity of the gel phase that makes the regular packing of the lipid bilayer more difficult as compared with the fluid phase, where the reorganization of the lipid layers is much easier for the loosely packed lipid molecules at elevated temperatures. Besides, for both samples (2/1 and 1/1), further cooling the sample to 20 °C, the same SAXS and WAXS profiles as those of the initial 20 °C can be obtained, suggesting that gel–fluid transitions of the samples are reversible, in good agreement with our DSC data.

Since the gel–fluid transitions were in a binary lipid mixtures, the phase state of the samples are composed of two lipid components. The single, sharp DSC peaks in Fig. 2 and 3A for the 2/1 and 1/1 samples indicate that the two components are miscible and can experience a highly cooperative transition upon heating.

Shown in Fig. 7 are the temperature-dependent SAXS (A and B) and WAXS (C) data for the DPPC/DODAB = 1/2 sample at a heating rate of 0.5 °C min^{-1}. At 20 °C, the average d value calculated from the SAXS peaks is 24.5 nm. When heating to 45 °C, the d value slightly changes to 24.2 nm. From the WAXS data (Fig. 7C), we can see that the sample at 20 °C shows several peaks at 10.5, 11.1, 12.0, 12.6, 13.6, 14.3 and 14.8 nm^{-1}. These peaks reflect the

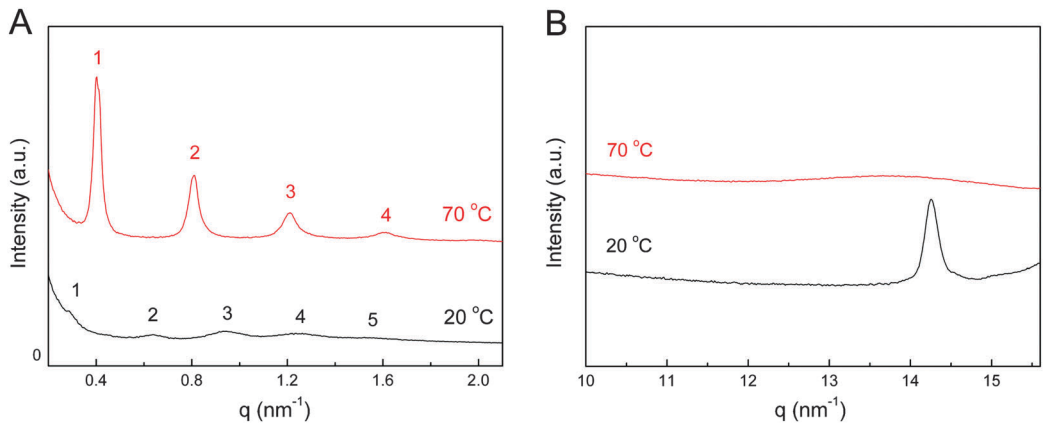

Fig. 6 SAXS (A) and WAXS (B) results of DPPC/DODAB = 1/1 (total lipid content = 25 wt%). Before measurements, these samples were first incubated at −20 °C for 2 days and then stored at 20 °C for 14 days.

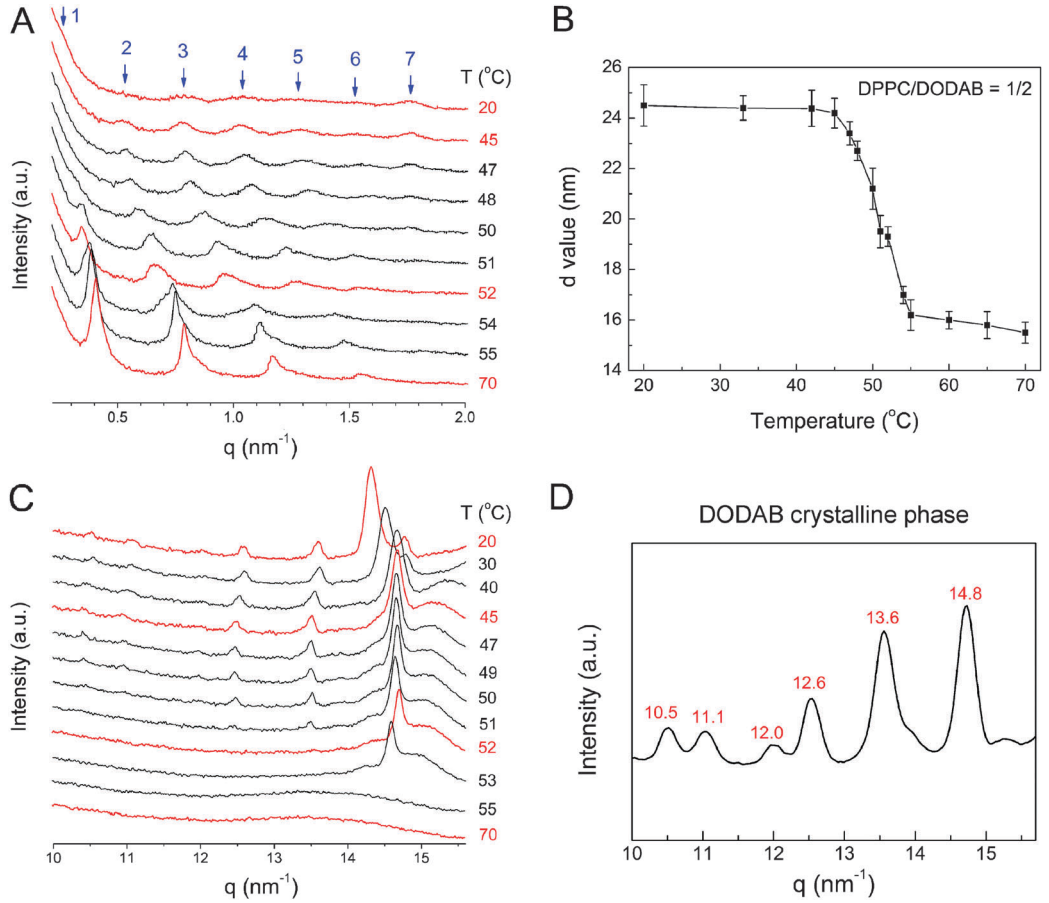

Fig. 7 SAXS (A and B) and WAXS (C) results of DPPC/DODAB = 1/2 (total lipid content = 25 wt%) at designed temperatures. Before measurements, the samples were first incubated at −20 °C for 2 days and then stored at 20 °C for 14 days. (D) The WAXS result of the crystalline phase of DODAB aqueous dispersion (25 wt%) at 20 °C. The preparation of the crystalline phase of DODAB can be found in the references.[41,42]

ordered tight packing of the lipid hydrocarbon tails. By careful comparison of these peaks with those of the crystalline phase of pure DODAB at 20 °C (Fig. 7D), we conclude that all these peaks except 14.3 nm^{-1} are from crystalline DODAB. The largest peak at 14.3 nm^{-1} (d = 0.44 nm) originates from the non-tilted gel-state DPPC. Upon increasing the temperature from 20 °C to 45 °C, we can see that the largest peak experiences evident changes in the peak shape and peak position, indicating changes in the rearrangement of the DPPC hydrocarbon tails. At 45 °C, the sharp peak at 14.7 nm^{-1} (d = 0.43 nm) and a broad shoulder on the high-angle side (at 15.2 nm^{-1}) arise from packing of the tilted hydrocarbon chains in a quasi-hexagonal lattice,[49,52,53] which are the typical characteristics of a tilted gel phase ($L_{\beta'}$) of the DPPC aggregates. The change in the WAXS peaks in this temperature range is consistent with the shallow exothermic peak observed in the DSC heating result for the DPPC/DODAB = 1/2 sample in Fig. 3A. Thus, at 45 °C, a DODAB-rich crystalline domain and a DPPC-rich gel domain coexist in the same bilayer, exhibiting a single repeat distance of 24.2 nm. When heated to above 50 °C, both the SAXS and WAXS data undergo significant changes. The repeat distance obtained from the SAXS peaks at 52 °C is 19.3 nm. The WAXS profile shows that the peaks from the crystalline DODAB vanish, leaving only the peaks from the tilted gel-state DPPC. Since the WAXS profile at 52 °C does not show any peaks from a gel-state DODAB (usually as a single sharp peak at q = 14.9 nm^{-1} or d = 0.42 nm),[54] we propose that at this temperature the DODAB-rich phase transforms into the fluid state, coexisting with the DPPC-rich gel domain. By further heating to 55 °C or higher, a very broad peak at 13.6 nm^{-1} (d = 0.46 nm) is seen, indicating that the gel-state DPPC-rich phase also melts to form a fluid phase. From the SAXS data we can obtain a repeat distance of 15.5 nm. Since the DPPC and DODAB molecules are both in a melted state, lateral diffusion can easily occur, thus we suppose that the DPPC and DODAB molecules are in a well-mixed state to reduce the electrostatic repulsions between the neighboring DODAB molecules and minimize the overall free energy of the system.

These WAXS data in Fig. 7C show that upon heating the DPPC/DODAB = 1/2 sample obtained after incubation at −20 °C for 2 days and 20 °C for 14 days, the DPPC molecules first undergo a further reorganization at the temperature range of 20 to 45 °C, and then the crystalline DODAB molecules in the DODAB-rich domain melt to a fluid state when the temperature is above 50 °C. Finally, upon further heating to 55 °C, the DPPC molecules in the DPPC-rich gel domain also melt to the

fluid phase.[55] The observed "shallow exothermic DSC peak" (Fig. 3A) corresponds to the structural reorganization of the DPPC molecules in the bilayer, and the two consecutive endothermic peaks at 51 °C and 54 °C (Fig. 3A) correspond to the "crystalline DODAB to fluid DODAB transition" and the "gel-state DPPC to fluid DPPC transition".

When the sample at 70 °C was cooled to 20 °C at −5 °C min^{-1}, the large sharp peak at 14.3 nm^{-1} (reflecting the packing tightness of the hydrocarbon tails) in the WAXS profile (data not shown) was seen. This suggests that the DPPC and DODAB molecules are both in the gel phase. The *d* value changes to 17.7 nm as evaluated from the SAXS results (data not shown). Considering the two endothermic peaks in the immediate reheating curve in Fig. 2C for the 1/2 sample, the results show that the 1/2 sample freshly cooled from 70 °C is in a mixed gel phase: a DODAB-rich gel domain and a DPPC–DODAB mixed gel domain, and the two endothermic peaks upon heating correspond to the melting of the two domains. Such assignments of the phase states are reasonable since the melting temperature of the latter (53 °C) is very close to those of the 2/1 and 1/1 samples (50 and 55 °C) whose DODAB content is 33 mol% and 50 mol%, respectively (Fig. 2C). The results indicate that the DODAB content in the DPPC–DODAB mixed gel domain may fall in the region of 33–50 mol%. Besides, the peak at 56 °C for the "−20 °C 2 days, 20 °C 30 days" sample is broader than the peaks at 56 °C in the other two curves in Fig. 2C, indicating different phase transition mechanisms: the former ("−20 °C 2 days, 20 °C 30 days") is due to the melting of the DPPC-rich gel domain while the latter ("immediate reheating" and "20 °C 30 days") is due to the melting of the DPPC–DODAB mixed gel domain. These results and analyses suggest that during the "−20 °C 2 days, 20 °C 30 days" treatment, some DODAB molecules are squeezed out from the DPPC–DODAB mixed domain, forming a DPPC-rich domain and a DODAB-rich domain where the DODAB molecules experience crystallization. The acceleration of the crystallization process of DODAB molecules at low temperature (−20 °C) has already been confirmed by our previous paper dealing with the phase behavior of neat DODAB dispersions.[42]

We have also performed conventional DSC experiments for the three d_{62}-DPPC–DODAB binary mixtures with the molar ratios of 2/1, 1/1 and 1/2 (Fig. 3B). The results will help explain the corresponding temperature-dependent FTIR data. We can see that the results are very similar to those of the DPPC–DODAB binary mixtures, except the small differences in the phase transition temperatures. The 2/1 and 1/1 samples show a single endothermic peak at 52 °C and 54 °C, respectively, while the 1/2 sample shows two endothermic peaks at 48 °C and 52 °C.

For the DPPC/DODAB = 1/2 sample, as has been mentioned for the dilute sample, the DODAB molecules can undergo crystallization after low temperature (−20 °C) incubation. To study the crystallization kinetics of the DODAB molecules in the concentrated sample, we carried out DSC experiments to examine the 25 wt% lipid sample that was cooled from 70 °C to 20 °C at −5 °C min^{-1} and incubated at 20 °C for different periods of time, and the results are shown in Fig. 4A. The immediate reheating scan shows two peaks at 43 °C and 56 °C. Similar to the dilute 1/2 sample that undergoes immediate reheating (Fig. 2C), these two peaks correspond to the melting of the DODAB-rich gel domain and the DPPC–DODAB mixed gel domain, respectively. After incubation at 20 °C for 135 min, a small shoulder-peak at 52 °C can be seen during heating, and the peak becomes larger as the incubation time increases. This peak is assigned to the melting of the DODAB-rich crystalline domain. After incubation of 72 h, the previous peak at 43 °C

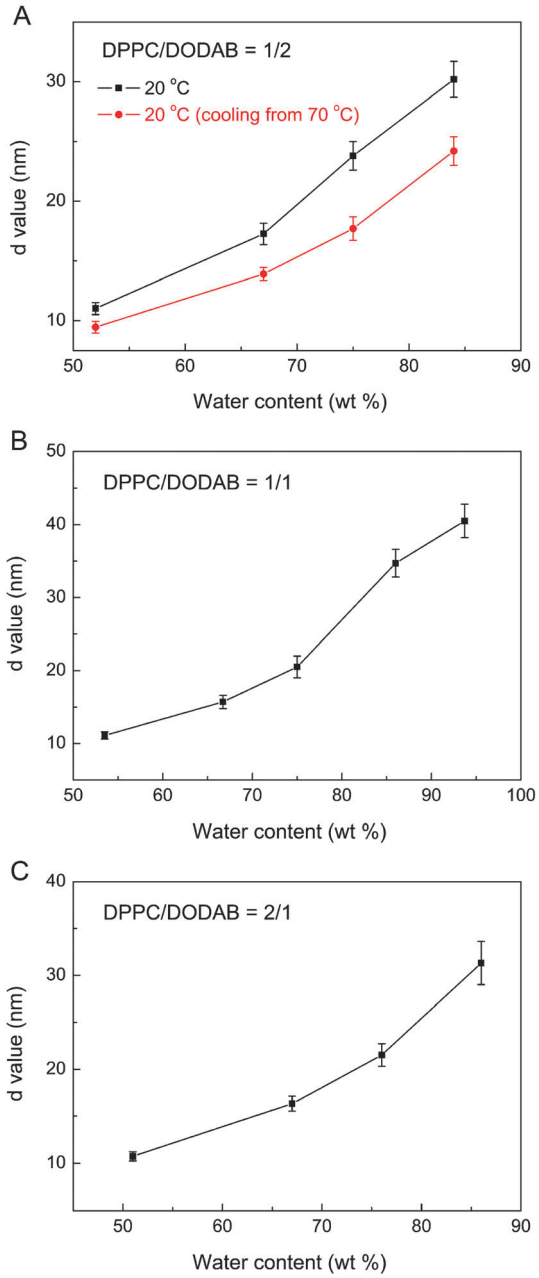

Fig. 8 Dependencies of the repeat distances (*d* values) on the water content at 20 °C (after incubation at −20 °C for 2 days and 20 °C for 14 days). (A) DPPC/DODAB = 1/2, (B) DPPC/DODAB = 1/1, and (C) DPPC/DODAB = 2/1. For DPPC/DODAB = 1/2, the *d* values obtained by cooling the samples from 70 °C to 20 °C (5 °C min^{-1}) were also given.

disappears and is completely replaced by the new peak at 52 °C, indicating the completion of the crystallization process during the incubation at 20 °C.

To examine the effect of the heating rate, the sample that had been cooled from 70 °C to 20 °C at −5 °C min^{-1} was heated to 65 °C at 0.5 °C min^{-1}. As can be seen in Fig. 4B, there is a shallow exothermic peak in the temperature range of 29 to 38 °C, similar to the case shown in Fig. 3A, indicating the crystallization of the DODAB molecules within the lipid mixtures during the slow heating process (0.5 °C min^{-1}). Such a crystallization process upon slow heating can be effectively avoided if a fast heating rate (5 °C min^{-1}) is applied (as shown in the immediate reheating scan in Fig. 4A). The tiny endothermic peak at 42 °C (marked with an arrow) indicates the presence of a residual DODAB-rich gel domain. If the sample that was cooled from 70 °C to 20 °C at −5 °C min^{-1} was incubated at 20 °C for 14 days, the heating scan shows two clear peaks at 51 °C and 54 °C. This suggests that the crystallization process has completed during the incubation.

We have also investigated the dependencies of the repeat distances (*d* values) of the three DPPC–DODAB binary mixtures at 20 °C (after incubation at −20 °C for 2 days and 20 °C for 14 days) on the water content of the samples (Fig. 8). Fig. 8A also shows the repeat distances of the DPPC/DODAB = 1/2 sample after cooling from 70 °C to 20 °C at 5 °C min^{-1}. The results show that for all the three mixtures the repeat distance increases with increasing water content. Besides, SAXS results of the DPPC/DODAB = 1/1 and 2/1 systems show that the addition of NaCl largely reduces the lipid repeat distances, which eventually reach a constant value of 6.3–6.4 nm above 250 mM NaCl (see Fig. 9). The results mean that the electrostatic repulsions are significantly screened by the added salts. A previous work carried out for dilute DPPC–DODAB vesicles (2 mM lipid concentration) showed that the 1/1 mixed DPPC/DODAB system had the highest colloidal stability against salt (1, 50 and 150 mM NaCl), and the vesicle size substantially increased upon increasing NaCl concentrations by decreasing intrabilayer electrostatic repulsion from screening of the surface charge.[45] The decreased intrabilayer electrostatic repulsion can cause a decrease in the membrane curvation, resulting in the formation of larger vesicles through vesicle aggregation or formation of multilamellar vesicles. While the present work showed that the addition of NaCl can screen the electrostatic repulsions between two adjacent bilayers (interbilayers) and decrease the repeat distances of the concentrated DPPC–DODAB multilamellar vesicles (25 wt%) for the 1/1 and also the 2/1 systems. The lipid concentration is very high in our case and thus no colloidal stability was evaluated.

3.2. FTIR spectroscopy

FTIR results can provide submolecular details of the various phase states of the binary mixtures. To study the rearrangements of the lipid tails of DPPC and DODAB molecules independently, the deuterated DPPC sample, d_{62}-DPPC, was used instead of the normal hydrogenated DPPC sample to prepare the lipid binary mixtures. Fig. 10 gives the dependencies of FTIR peak positions of ν_sCH_2 (the symmetric stretching vibration of CH_2 in the lipid tail region) in DODAB and ν_sCD_2 (the symmetric stretching vibration of CD_2 in the lipid tail region) in d_{62}-DPPC on temperature for the three samples with the DPPC/DODAB molar ratios of 1/2, 1/1 and 2/1 after incubation at −20 °C for 2 days and 20 °C for 14 days. For the "1/2" sample (Fig. 10A), we can see that upon heating, the peak position of ν_sCH_2 in DODAB shifts away from the general trend at above 40 °C, and this turns to be much evident at 45 °C. The peak position reaches a plateau when the temperature reaches 53 °C. For ν_sCD_2 in d_{62}-DPPC, the starting point is around 45 °C, and a sharp transition occurs at 50 °C. The shifts towards high frequencies indicate that the CH_2 chains of DODAB and the CD_2 chains in d_{62}-DPPC change from an all-*trans* conformation in the crystalline/gel phases at 20 °C to a state with increased *gauche* conformers in the fluid phase at 65 °C.[48,56–60] More importantly, the results show that DODAB melts earlier than d_{62}-DPPC, which agrees well with the DSC data of d_{62}-DPPC/DODAB = 1/2 sample (Fig. 3B) that it is the crystalline DODAB molecules in the DODAB-rich phase that convert to the fluid phase first, at around 40 °C. For the d_{62}-DPPC/DODAB = 1/1 and 2/1 samples (Fig. 10B and C), ν_sCH_2 and ν_sCD_2 change simultaneously, which suggests that the two lipids are well miscible with each other.

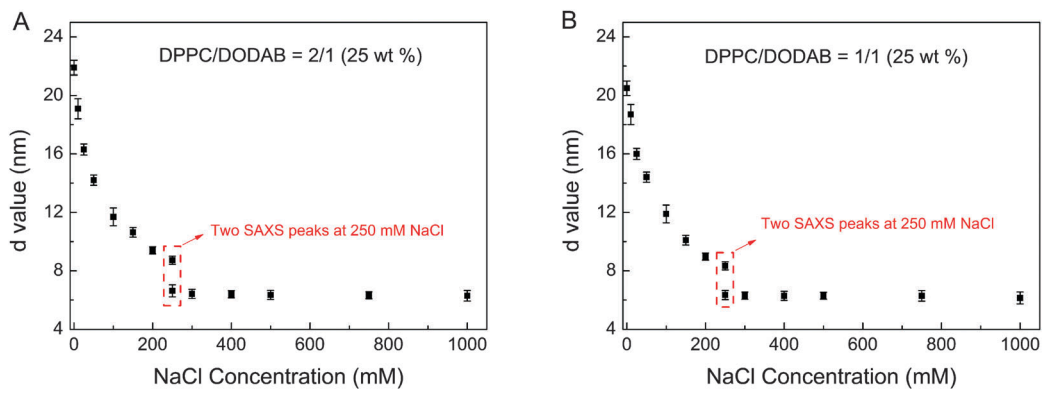

Fig. 9 Dependencies of the repeat distances (*d* values) on NaCl concentration at 20 °C obtained from SAXS experiments. (A) DPPC/DODAB = 2/1, (B) DPPC/DODAB = 1/1.

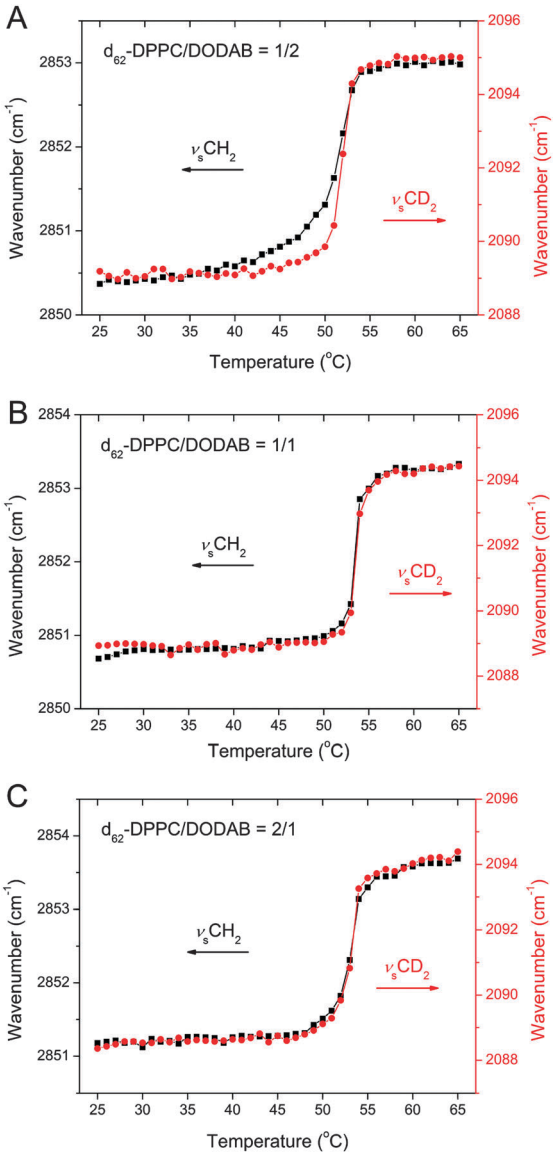

Fig. 10 Dependencies of FTIR peak positions of $\nu_s CH_2$ in DODAB and $\nu_s CD_2$ in d_{62}-DPPC on temperature in d_{62}-DPPC–DODAB mixtures (total lipid content = 25 wt%). (A) d_{62}-DPPC/DODAB = 1/2, (B) d_{62}-DPPC/DODAB = 1/1, and (C) d_{62}-DPPC/DODAB = 2/1. Before measurements, these samples were first incubated at −20 °C for 2 days and then stored at 20 °C for 14 days.

3.3. Demixing and crystallization in DPPC–DODAB mixtures

Fig. 11 summarizes the main findings of the present work. For the DPPC/DODAB = 1/2 sample (Fig. 11A), when it is cooled from a mixed fluid phase at 70 °C to 20 °C at 5 °C min^{-1}, a phase-separated, mixed gel state consisting of a DODAB-rich gel domain and a DPPC–DODAB mixed gel domain forms. The DODAB-rich domain will first convert to a fluid phase when the temperature goes above 44 °C. Upon further heating to 70 °C, both of the two domains melt, and a mixed fluid phase is obtained. If the mixed gel state is incubated at 20 °C for 14 days and heated slowly (0.5 °C min^{-1}) to 45 °C, as revealed by the WAXS data in Fig. 7C, the DODAB molecules will be excluded from the DPPC–DODAB mixed domain and crystallized, leading to the formation of a domain rich in tilted gel DPPC and a domain rich in crystalline DODAB. Upon heating to 52 °C, the crystalline DODAB first melts (as evidenced by the FTIR data in Fig. 10A), resulting in the coexistence of a DODAB-rich fluid domain and a DPPC-rich gel domain. Finally, heating to 70 °C results in the formation of a mixed fluid state. DPPC/DODAB = 1/1 and 2/1 samples (Fig. 11B and C) undergo reversible mixed gel to mixed fluid phase transformations upon heating and cooling, regardless of which sample pretreatment procedures (“immediate reheating”, “20 °C 30 days”, or “−20 °C 2 days, 20 °C 30 days”) were applied.

As in our present system consisting of the neutral DPPC and positively charged DODAB, the interbilayer repulsive interactions include electrostatic, hydration, and undulation forces, while the interbilayer attractive interaction is the van der Waals force. Among the repulsive forces, the undulation force (which is regarded as the steric interactions caused by collision of bilayers) is considered to take effect when the water layer is reduced.[61,62] The hydration force (mainly due to the difficulty in removing the structured water between lipid bilayers when two opposing membrane surfaces come close) assumes greater significance as the bilayers come into closer proximity.[63,64] Considering that in our systems the bilayers are separated by a very large distance (with the interlamellar water layer thickness of 10–20 nm), the repulsive hydration and undulation forces are incidental. Thus, the most important repulsive force is the electrostatic interaction. As the electrostatic force for the neutral DPPC is negligible,[65] the dominant repulsive interaction is from the positively charged headgroups of DODAB. The continuous swelling of the lipid repeat distance shows that even at the maximum water content that has been investigated in this work, the attractive force does not balance the repulsive. However, the results shown in Fig. 9 suggest that high salt concentrations (above 250 mM NaCl) can screen the electrostatic repulsions and reduce the repeat distances to a constant value (6.3–6.4 nm).

The present work indicates that when DODAB is not in excess (the content of DODAB is not higher than 50 mol%), DPPC is miscible with DODAB. The neat DODAB molecules in aqueous media are easy to crystallize at high concentrations (*e.g.*, above 6.7 wt%),[42] this means that addition of enough DPPC to DODAB hinders the crystallization of DODAB as in the samples with the molar ratios of DPPC/DODAB = 2/1 and 1/1. However, when DODAB is in excess, such as for the sample with the DPPC/DODAB molar ratio of 1/2, DODAB can crystallize in both the concentrated and diluted samples. In the mixed DPPC/DODAB domains of the three binary mixtures (1/1, 2/1 and 1/2), the presence of the cationic DODAB can alter the orientation of the P–N (phosphorous–nitrogen) dipole vector of DPPC from more parallel to more perpendicular to the membrane plane (as shown in Fig. 11), since neat DPPC molecules are packed with the P–N dipole vector more parallel to the membrane plane. In such a conformation, the $N(CH_3)_2^+$ groups of DODAB act as “glue” to bind with the PO_4^- groups of DPPC through electrostatic interactions, which can significantly increase the “cooperativity” of the melting process of

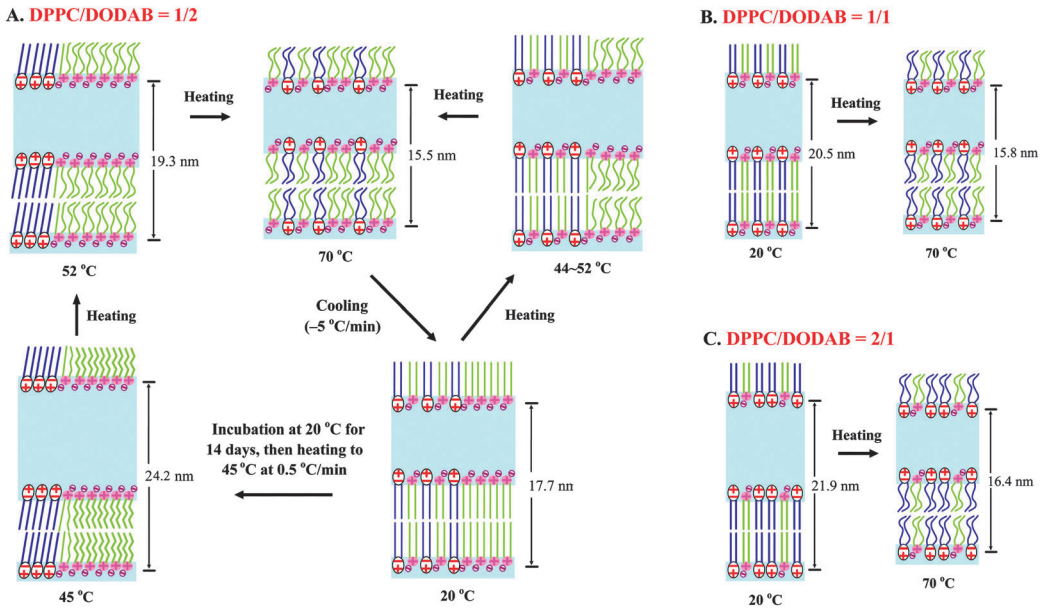

Fig. 11 Schematic models showing the phase transformations of the three DPPC–DODAB systems. (A) DPPC/DODAB = 1/2, (B) DPPC/DODAB = 1/1 and (C) DPPC/DODAB = 2/1. In (A), for conciseness, only DPPC molecules or DODAB molecules are depicted in the DPPC-rich or DODAB-rich domains.

the mixed DPPC–DODAB domain. As a result, a sharper DSC endothermic peak was observed for the melting of the mixed DPPC–DODAB domain as compared with the melting of the DPPC-rich gel domain. These intermolecular interactions between DPPC and DODAB in mixed DPPC–DODAB domains can explain why the insertion of DPPC within the array of DODAB molecules can hinder the crystallization of DODAB. Besides, they can also well explain the observed different DSC peak widths of the second endothermic peaks for the DPPC/DODAB = 1/2 sample after different treatments performed in Fig. 2C, where the peak at T_{onset} = 53 °C for the ''immediate reheating'' and ''20 °C 30 days'' samples corresponds to the melting of the mixed DPPC–DODAB region, while the peak at T_{onset} = 52 °C corresponds to the melting of a DPPC-rich gel state domain for the ''−20 °C 2 days, 20 °C 30 days'' curve. Further, the change in the orientation of the P–N dipole vector of DPPC can also cause a tighter packing of the lipid acyl tails, and thus the conversion from the gel-state DPPC to fluid-state DPPC occurs at a higher temperature in all the 1/1, 1/2 and 2/1 DPPC–DODAB mixtures, as compared with the gel–fluid transition temperature (∼42 °C) of the neat DPPC dispersions.[49,52]

Another very interesting and important result is that the crystallized DODAB molecules in the phase separated DPPC/DODAB = 1/2 system still remain in the same lipid bilayer. If the crystalline DODAB molecules were excluded from the bilayer and existed as separate crystalline aggregates, the lamellar repeat distance would be 3.7 nm, as revealed by our previous work.[41] Actually, the equally separated symmetric SAXS peaks at 40 °C in Fig. 5A show that only one repeat distance exists in the mixed binary system. We thus assume that the crystallized DODAB molecules exist together with the DPPC-rich gel medium in the same bilayer, and the large hydration degree needed for the gel-state DODAB molecules in the DPPC-rich gel domain makes the release of Br^- ions of DODAB into aqueous solution possible. The resultant net positive surface charge renders the swelling of the lipid bilayers.

The crystallization mechanism of the neat DODAB dispersion has been investigated in a previous work.[41] It was found that the fluid phase of DODAB converts to the crystalline (coagel) phase upon cooling *via* a two-step mechanism: first to the gel phase upon cooling and then to the crystalline phase. As evidenced by the FTIR results, the nucleation step involves the ordering of the hydrocarbon tails and a partial dehydration in the headgroups of DODAB molecules. The crystallization is based on rapidly cooling the sample, and the rearrangements occur spontaneously and randomly throughout the dispersion, which can be regarded as a homogeneous nucleation process. Regarding the mechanism of DODAB crystallization in the DPPC/DODAB (1/2) mixture after the ''−20 °C 2 days and 20 °C 30 days'' treatment, since the crystallization of DODAB within the DODAB-rich gel domain needs a supercooling procedure (−20 °C, 2 days) to make the initial nuclei easy to form. The further incubation at an elevated temperature (20 °C, 30 days) accelerates the growth of these initial nuclei. This is a characteristic of homogenous crystallization. The formation of the DODAB-rich domain is due to the different intermolecular forces and the relative content of the two lipid components. In the DPPC/DODAB (2/1 and 1/1) mixtures, DODAB is not a dominant component and the two lipids can mix well with each other, producing a DPPC–DODAB mixed gel phase without the formation of two phase-separated domains. Thus upon cooling to a low temperature and/or long-time room temperature incubation, the strong intermolecular interactions between DPPC and DODAB cannot be destroyed and no DODAB-rich nucleation sites can be formed under these conditions. This may account for the results that no crystallization

of DODAB occurs in DPPC/DODAB (1/1) and DPPC/DODAB (2/1) samples.

Finally, since both of the two molecules, DPPC and DODAB, are only ~3 nm in molecular length, the observed very large repeat distances of the DPPC–DODAB binary mixtures in water indicate a very large thickness of the water layer. Such a large water layer may have potential abilities to incorporate various bioactive molecules such as DNA, proteins, and drugs. The DPPC–DODAB system can also be used to study how DNA, proteins, charged polymers/polyelectrolyte, and small nanoparticles diffuse into the large interbilayer region. These systems enable us to fabricate functional biomaterials (such as biofilms and multilamellar liposomes or nanostructures), and can also be used as good platforms for fundamental biophysical or colloidal studies.

4. Conclusions

Our present work shows that the molar ratio between two lipid components is crucial for determining the demixing and crystallization of one lipid component within the lipid binary mixture. For example, the 1/1 and 2/1 DPPC/DODAB mixtures (1 mg mL^{-1} and 25 wt% samples) are very stable under various conditions, and the two systems undergo reversible gel–fluid phase transitions upon heating and cooling, and no crystalline phases form. When DODAB molecules are dominant in the mixture (the 1/2 mixed sample), cooling the homogeneous fluid phase results in the formation of two coexisting gel phases: a DODAB-rich gel domain and a DPPC–DODAB mixed gel (non-tilted) domain. The subsequent crystallization process results in further demixing to reach a phase-separated state consisting of a DODAB-rich crystalline domain and a DPPC-rich tilted gel domain. Besides, all the experimental evidence supports the understanding that the crystallized DODAB-rich domain remains in the same lipid bilayer as the DPPC-rich domain.

FTIR results provide submolecular details of the phase transformation: the DPPC and DODAB molecules undergo cooperative structural rearrangements in the 1/1 and 2/1 mixed DPPC/DODAB samples upon heating. For the 1/2 mixed DPPC/DODAB system, the melting of the DODAB-rich domain (crystalline DODAB to fluid DODAB) is prior to the melting of the DPPC-rich domain (tilted gel DPPC to fluid DPPC). Finally, for the 1/1 sample, the *d* value is found to depend strongly on the water content and salt concentration. A higher water content results in a larger *d* value, while a higher salt concentration leads to a smaller *d* value. The present investigation on the phase stability and phase separation of the zwitterionic–cationic lipid binary mixtures may help to explain the various fundamental phenomena observed in the studies of their monolayer, bilayer and vesicular systems.

Acknowledgements

This work was supported by grants from the Natural Science Foundation of China (NSFC: Grant No. 21133009, 21273130 and 21303017) and the Natural Science Foundation of Jiangsu Province (KB20130601). The SAXS and WAXS data were collected at the beamline BL16B1 of the Shanghai Synchrotron Radiation Facility (SSRF) with the assistance of the station scientists. We also appreciate the insightful discussions with Prof. Peter J. Quinn at the Department of Biochemistry, King's College London.

Notes and references

1 P. L. Felgner, T. R. Gadek, M. Holm, R. Roman, H. W. Chan, M. Wenz, J. P. Northrop, G. M. Ringold and M. Danielsen, *Proc. Natl. Acad. Sci. U. S. A.*, 1987, **84**, 7413.
2 P. L. Felgner and G. M. Ringold, *Nature*, 1989, **337**, 387.
3 R. Koynova and R. C. MacDonald, *Nano Lett.*, 2004, **4**, 1475.
4 G. Caracciolo, D. Pozzi, H. Amenitsch and R. Caminiti, *Langmuir*, 2006, **22**, 4267.
5 R. Koynova and B. Tenchov, *Soft Matter*, 2009, **5**, 3187.
6 T. Neumann, S. Gajria, M. Tirrell and L. Jaeger, *J. Am. Chem. Soc.*, 2009, **131**, 3440.
7 T. Neumann, S. Gajria, N. F. Bouxsein, L. Jaeger and M. Tirrell, *J. Am. Chem. Soc.*, 2010, **132**, 7025.
8 R. Koynova and B. Tenchov, *Top. Curr. Chem.*, 2010, **296**, 51.
9 R. Koynova, *Methods Mol. Biol.*, 2010, **606**, 399.
10 Y. Lu, S. X. Hu and M. Li, *Langmuir*, 2010, **26**, 3539.
11 J. O. Rädler, I. Koltover, T. Salditt and C. R. Safinya, *Science*, 1997, **275**, 810.
12 I. Koltover, T. Salditt, J. O. Rädler and C. R. Safinya, *Science*, 1998, **281**, 78.
13 G. Caracciolo, D. Pozzi, H. Amenitsch and R. Caminiti, *Langmuir*, 2005, **21**, 11582.
14 G. Caracciolo, C. Marchini, D. Pozzi, R. Caminiti, H. Amenitsch, M. Montani and A. Amici, *Langmuir*, 2007, **23**, 4498.
15 G. Caracciolo, D. Pozzi, R. Caminiti, G. Mancini, P. Luciani and H. Amenitsch, *J. Am. Chem. Soc.*, 2007, **129**, 10092.
16 S. W. Hui, M. Langner, Y. L. Zhao, P. Ross, E. Hurley and K. Chan, *Biophys. J.*, 1996, **71**, 590.
17 S. May, D. Harries and A. Ben-Shaul, *Biophys. J.*, 2000, **78**, 1681.
18 I. S. Zuhorn, V. Oberle, W. H. Visser, J. B. F. Engberts, N. U. Bakowsky, E. Polushkin and D. Hoekstra, *Biophys. J.*, 2002, **83**, 2096.
19 A. M. Carmona-Ribeiro, *Curr. Med. Chem.*, 2003, **10**, 2425.
20 S. Ristori, J. Oberdisse, I. Grillo, A. Donati and O. Spalla, *Biophys. J.*, 2005, **88**, 535.
21 D. Hirsch-Lerner, M. Zhang, H. Eliyahu, M. E. Ferrari, C. J. Wheeler and Y. Barenholz, *Biochim. Biophys. Acta*, 2005, **1714**, 71.
22 E. C. Mbamala, A. Fahr and S. May, *Langmuir*, 2006, **22**, 5129.
23 S. Zhang, Y. Zhao, B. Zhao and B. Wang, *Bioconjugate Chem.*, 2010, **21**, 1003.
24 F. Domenici, C. Castellano, F. Dell'Unto, A. Albinati and A. Congiu, *Colloids Surf., B*, 2011, **88**, 432.
25 B. Ma, S. Zhang, H. Jiang, B. Zhao and H. Lv, *J. Controlled Release*, 2007, **123**, 184.
26 W. L. Hsu, Y. C. Li, H. L. Chen, W. Liou, U. S. Jeng, H. K. Lin, W. L. Liu and C. S. Hsu, *Langmuir*, 2006, **22**, 7521.
27 R. Koynova, L. Wang and R. C. MacDonald, *Proc. Natl. Acad. Sci. U. S. A.*, 2006, **103**, 14373.

28 C. H. Chang, C. H. Liang, Y. Y. Hsieh and T. H. Chou, *J. Phys. Chem. B*, 2012, **116**, 2455.
29 R. Zantl, F. Artzner, G. Rapp and J. O. Rädler, *Europhys. Lett.*, 1999, **45**, 90.
30 A. A. Gurtovenko, M. Patra, M. Karttunen and I. Vattulainen, *Biophys. J.*, 2004, **86**, 3461.
31 W. Zhao, A. A. Gurtovenko, I. Vattulainen and M. Karttunen, *J. Phys. Chem. B*, 2012, **116**, 269.
32 A. L. Troutier, L. Véron, T. Delair, C. Pichot and C. Ladavière, *Langmuir*, 2005, **21**, 9901.
33 V. Levadny and M. Yamazaki, *Langmuir*, 2005, **21**, 5677.
34 T. A. Spurlin and A. A. Gewirth, *J. Am. Chem. Soc.*, 2007, **129**, 11906.
35 L. F. Zhang, T. A. Spurlin, A. A. Gewirth and S. Granick, *J. Phys. Chem. B*, 2006, **110**, 33.
36 A. M. Carmona-Ribeiro, *J. Phys. Chem.*, 1992, **96**, 9555.
37 A. M. Carmona-Ribeiro, *Chem. Soc. Rev.*, 1992, **21**, 209.
38 A. M. Carmona-Ribeiro, *Chem. Soc. Rev.*, 2001, **30**, 241.
39 A. M. Carmona-Ribeiro, *Curr. Med. Chem.*, 2006, **13**, 1359.
40 M. Kodama, T. Kunitake and S. Seki, *J. Phys. Chem.*, 1990, **94**, 1550.
41 F. G. Wu, N. N. Wang and Z. W. Yu, *Langmuir*, 2009, **25**, 13394.
42 F. G. Wu, Z. W. Yu and G. Ji, *Langmuir*, 2011, **27**, 2349.
43 A. M. Gonçalves da Silva and R. I. S. Romão, *Chem. Phys. Lipids*, 2005, **137**, 62.
44 F. M. Linseisen, S. Bayerl and T. M. Bayerl, *Chem. Phys. Lipids*, 1996, **83**, 9.
45 C. N. C. Sobral, M. A. Soto and A. M. Carmona-Ribeiro, *Chem. Phys. Lipids*, 2008, **152**, 38.
46 A. M. Carmona-Ribeiro and T. M. Herrington, *J. Colloid Interface Sci.*, 1993, **156**, 19.
47 S. P. Moura and A. M. Carmona-Ribeiro, *J. Colloid Interface Sci.*, 2007, **313**, 519.
48 F. G. Wu, L. Chen and Z. W. Yu, *J. Phys. Chem. B*, 2009, **113**, 869.
49 F. G. Wu, Q. Jia, R. G. Wu and Z. W. Yu, *J. Phys. Chem. B*, 2011, **115**, 8559.
50 M. Nadler, A. Steiner, T. Dvir, O. Szekely, P. Szekely, A. Ginsburg, R. Asor, R. Resh, C. Tamburu, M. Peres and U. Raviv, *Soft Matter*, 2011, **7**, 1512.
51 B. F. Qiao and M. Olvera de la Cruz, *J. Phys. Chem. B*, 2013, **117**, 5073.
52 Z. W. Yu and P. J. Quinn, *Biophys. J.*, 1995, **69**, 1456.
53 F. G. Wu, N. N. Wang, L. F. Tao and Z. W. Yu, *J. Phys. Chem. B*, 2010, **114**, 12685.
54 P. Saveyn, P. Van der Meeren, M. Zackrisson, T. Narayanan and U. Olsson, *Soft Matter*, 2009, **5**, 1735.
55 The melting of the DPPC molecules in the DPPC-rich gel domain is more difficult as compared to the neat DPPC molecules, since these DPPC molecules are mixed with some residual DODAB molecules and are confined within the surrounding DODAB-rich domains. This may help explain the higher transition temperature of the DPPC-rich gel domain as compared to that of the neat DPPC gel phase at around 42 °C.
56 F. G. Wu, J. J. Luo and Z. W. Yu, *Langmuir*, 2010, **26**, 12777.
57 F. G. Wu, N. N. Wang, J. S. Yu, J. J. Luo and Z. W. Yu, *J. Phys. Chem. B*, 2010, **114**, 2158.
58 F. G. Wu, J. S. Yu, S. F. Sun and Z. W. Yu, *Langmuir*, 2011, **27**, 14740.
59 F. G. Wu, N. N. Wang, Q. G. Zhang, S. F. Sun and Z. W. Yu, *J. Colloid Interface Sci.*, 2012, **374**, 197.
60 F. G. Wu, J. S. Yu, S. F. Sun, H. Y. Sun, J. J. Luo and Z. W. Yu, *Langmuir*, 2012, **28**, 7350.
61 H. I. Petrache, N. Gouliaev, S. Tristram-Nagle, R. T. Zhang, R. M. Suter and J. F. Nagle, *Phys. Rev. E: Stat. Phys., Plasmas, Fluids, Relat. Interdiscip. Top.*, 1998, **57**, 7014.
62 W. Helfrich, *Z. Naturforsch.*, 1978, **33a**, 305.
63 T. J. McIntosh and S. A. Simon, *Annu. Rev. Biophys. Biomol. Struct.*, 1994, **23**, 27.
64 M. L. Berkowitz, D. L. Bostick and S. Pandit, *Chem. Rev.*, 2006, **106**, 1527.
65 U. Vierl, L. Löbbecke, N. Nagel and G. Cevc, *Biophys. J.*, 1994, **67**, 1067.

